

Worst-Case Scenarios and Epidemics

G. Chowell and C. Castillo-Chavez

Center for Nonlinear Studies

Los Alamos National Laboratory

Los Alamos, NM 87545

&

Biological Statistics and Computational Biology

Cornell University

Ithaca, NY 14853

March 18, 2003

Abstract

Contingency plans and policies associated with the deliberate release of biological agents must be developed in the absence of data. Hence, the identification of landscapes that facilitate “worst” epidemics (worst-case scenarios) is essential. Common sense suggest

that “worst” epidemics are most likely to occur in populations where individuals mix randomly (proportionate mixing). Here, SIR (susceptible-infective-recovered) epidemics that result from the introduction of single or multiple sources are studied on various topologies including small-world and scale-free networks. A simple algorithm is used to compute the average growth rate during the initial exponential growth phase of the epidemic. This rate is used to estimate the severity of a single outbreak. In small-world networks, the average rate of epidemic growth is measured on the full spectrum of the disorder parameter $p \in [0, 1]$. Simulations show that the average rate of growth increases in a nonlinear fashion as the disorder in the network increases. Not surprisingly, the average rate of growth is higher when the initial infective source is placed in the most connected node (pressure point) than when it is randomly placed. The average rate of initial growth is also a non-decreasing function of the (small) number of initial infectious sources. Simulation results support the view that, worst-case epidemics, in small-world networks, occur when the outbreak begins at a few places and when $p = 1$ (random mixing). Simulation results also show that worst-case epidemics, on scale-free networks, are primarily driven by the network hierarchy, that is, sources placed on the most connected nodes have the biggest effect. Finally, simulations suggest that a significantly higher average rate of epidemic growth is observed in scale-free than in small-world networks. Hence, scale-free topologies may provide the “best” landscapes for the theoretical study of worst-case epidemics.

1 Introduction

The potential deliberate release of biological agents such as small-pox, influenza, or foot and mouth disease (FMD) is a source of continuous concern. It is believed that “worst” epidemics (single outbreaks) are most likely to occur in populations where individuals mix randomly (proportionate mixing). Therefore, the definition and identification of landscapes or topologies that support worst-case scenarios is critical. Here, SIR (susceptible-infective-recovered) epidemics that result from the introduction of single or multiple infectious sources are studied on various topologies including small-world and scale-free networks.

Most of the models studied in classical mathematical epidemiology fall in the class of *compartmental models* because the population under consideration is divided into classes or compartments defined by epidemiological status [2]. The simplest version assumes that individuals mix uniformly (*homogeneous mixing*) within each compartment. The study of the transmission dynamics of communicable diseases in human populations via mathematical (compartmental) models can be traced back to the work of Kermack and Mackendrick (1927). Their simple SIR (Susceptible-Infective-Removed) epidemic model (Figure 1) was not only capable of generating realistic single-epidemic outbreaks but also provided important theoretical epidemiological insights.



Figure 1: Simple SIR epidemic model.

The Kermack and Mackendrick (K-M) model in essence captures the theoretical underpinnings associated with the framework that it is currently used to define (and model) worst-case epidemic outbreaks. The K-M model is given by the following system of nonlinear differential equations

$$\begin{aligned}\dot{S} &= -\lambda(N)SI, \\ \dot{I} &= \lambda(N)SI - \gamma I, \\ \dot{R} &= \gamma I,\end{aligned}\tag{1}$$

where $S(t)$ denotes susceptible individuals at time t ; $I(t)$ infected (assumed infectious) individuals at time t ; $R(t)$ recovered (assumed permanently immune) individuals at time t ; $\lambda(N)$ the transmission rate when the total population is $N(N = S + I + R)$; and γ the recovery rate. In the case of a fatal disease, $N = S + I$ as $R(t)$ would denote those removed by death and γ the per-capita death rate.

The Kermack and Mackendrick threshold theorem establishes (quantitatively) the conditions required for successful disease invasion. This threshold theorem says that a disease will invade whenever its basic reproductive number

$$R_o = \frac{\lambda(N(0))N(0)}{\gamma} > 1.$$

R_o is interpreted as the number of secondary infectious individuals generated by a “typical”

infectious individual when introduced into a fully susceptible population ([4, 5]). An alternative interpretation is that, in a randomly mixing population, a disease will invade if there are enough susceptibles, that is, if

$$N(0) > \frac{\gamma}{\lambda(N(0))}.$$

Typically, it has been assumed that either $\lambda(N) = \frac{\beta_o}{N}$ or $\lambda(N) = \beta_o$ and, consequently, the interpretation of R_o depends on the definition of $\lambda(N)$ ([1, 2, 4]).

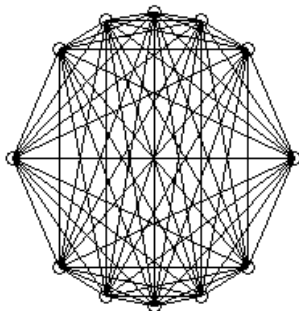


Figure 2: Fully-mixed transmission network.

Nold [6] introduced the concept of *proportionate mixing* as a way of modeling a simple form of heterogenous mixing. She divided the population into K groups each with population size $N_i(t) = S_i(t) + I_i(t) + R_i(t)$, ($i = 1, \dots, K$) and modeled an SIR epidemic that considered interactions of various intensities among individuals. In order to describe her framework we introduce the mixing matrix $P(t) = (P_{ij}(t))$ where $P_{ij}(t)$ denotes the proportion of contacts of individuals in group i with individuals in group j given that i -individual had a contact with

a member of the population at time t . Nold's proportionate mixing corresponds to the case where P_{ij} is independent of i , that is,

$$P_{ij} \equiv \bar{P}_j = \frac{C_j N_j}{\sum_{l=1}^k C_l N_l}, \quad (\text{II}) \quad (2)$$

where C_l denotes the average activity level (contact rate) of individuals in group $l = 1, \dots, k$. Other forms of mixing can be found in [4, 7, 8, 9] and references therein.

A slightly modified version of Nold's generalization of the Kermack-Mackendrick model (assumes that $\lambda_j \equiv \frac{\beta_j}{N_j}$, $j = 1, \dots, K$) is given by

$$\begin{aligned} \dot{S}_i &= -S_i(t) \sum_{j=1}^k \beta_j \bar{P}_j \frac{I_j}{N_j}, \\ \dot{I}_i &= S_i(t) \sum_{j=1}^k \beta_j \bar{P}_j \frac{I_j}{N_j} - \gamma_i I_i, \\ \dot{R}_i &= \gamma_i I_i, \quad i = 1, \dots, K \end{aligned} \quad (3)$$

Examples of mathematical studies for compartmental models of this type can be found in [1, 2, 4], and [6]. Extensions of these models to (local) populations interconnected via migrating individuals (*metapopulation models*) have been carried out in some situations (see [9] and references therein). In the K-M model and Nold's models, individuals mix at random (see Figure 2), an *uncommon* and extreme situation. Recent analyses of worst-case scenarios, for

the deliberate release of biological agents (smallpox in particular), have been carried out under the assumption that random mixing supports the worst epidemic outbreaks [14]. The focus of this paper (as suggested to us by Ed Kaplan) consists on the preliminary examination of the validity of this assumption.

The identification of worst-case scenarios would require an approach that considers “all” measures of mixing ([6]). The study of the meaning of worst-case scenarios using “mean” field models like the K-M or Nold’s model is problematic (mixing assumes a predetermined number of groups or types). Hence, we look at this question in the context of simple individual-based models where mixing is embedded in a preselected (fixed) topology. This approach also has its limitations as the nodes (individuals) of the network have no dynamics. However, we feel that this approach is useful if the goal is to study the “strength” of a single epidemic outbreak, that is, in the study of situations where transient disease dynamics are critical.

2 Individual-based models

Population structures are often represented by networks (graphs) composed of nodes (individuals) and edges (representing predefined relationships between nodes). Examples include family trees, traffic networks that describe street intersections by nodes and traffic direction by arrows (edges), and airline traffic networks. Graphs (networks) can be represented by the adjacency matrix T where $T(i, j) = 1$ implies that vertex i is connected to j . If the network is undirected (edges have no direction) then T is symmetric, that is, $T = T^t$ (transpose of T). An *adjacency list*, a compilation of the vertices of a graph and the vertices adjacent to such a vertex, is also

used to represent graphs. The analysis of network models can be traced back to the work of Erdős and Rényi in the 1960's. These researchers introduced the following simple algorithm for the construction of *random* networks ([16]): start with a fixed number of disconnected nodes N and connect each pair of nodes independently by an edge with probability p_{ER} . Hence, $p_{ER} = 0$ corresponds to the case where no node is connected to any of the other $N - 1$ nodes while $p_{ER} = 1$ corresponds to the case where every node is connected to all other nodes in the network (complete graph). The total number of edges when $p_{ER} = 1$ is $\binom{N}{2}$; the average number of edges is $\frac{N(N-1)p_{ER}}{2}$; and, the average degree of a node (number of edges incident from a node) is $z = (N - 1)p_{ER} \simeq Np_{ER}$ (for large N).

Erdős and Rényi [16] showed that for large systems (large N) the probability that a node has k edges follows the Poisson distribution $P(k) = \frac{\exp(-z)z^k}{k!}$, ($k = 0, 1, \dots, N$). Furthermore, they showed that there is a critical value of z (z_c) such that whenever $z > z_c$, a *connected component* (a subset of vertices in the graph each of which is reachable from the others by some path through the network) forms. Such component is often referred as the *spanning cluster* [38]. The Erdős and Rényi random graph provides a null-model for the “comparative” study of the disease transmission on other network topologies. The case $p_{ER} = 1$ (totally connected network) is naturally believed to be the generator of the landscape most conducive to disease spread and, in some sense, “corresponds” to Nold’s version of the K-M model. Hence, here we address, via simulations, whether or not in populations modeled by *comparable* graphs to those of Erdős and Rényi model support the worst possible epidemics. It is not clear, however,

whether or not, diseases spread at a faster rate in highly-clustered networks, that is, in networks where there is a higher probability that neighbors of a particular node are also neighbors of each other. The importance of this possibility comes in part, from the fact that Watts and Strogatz (1998) [19] showed that networks with high degree of aggregations (clustering), a characteristic absent in random networks (see Erdős and Rényi, [16]), are not uncommon. In order to explain our simulations of epidemics in various network setups, we need to describe their construction.

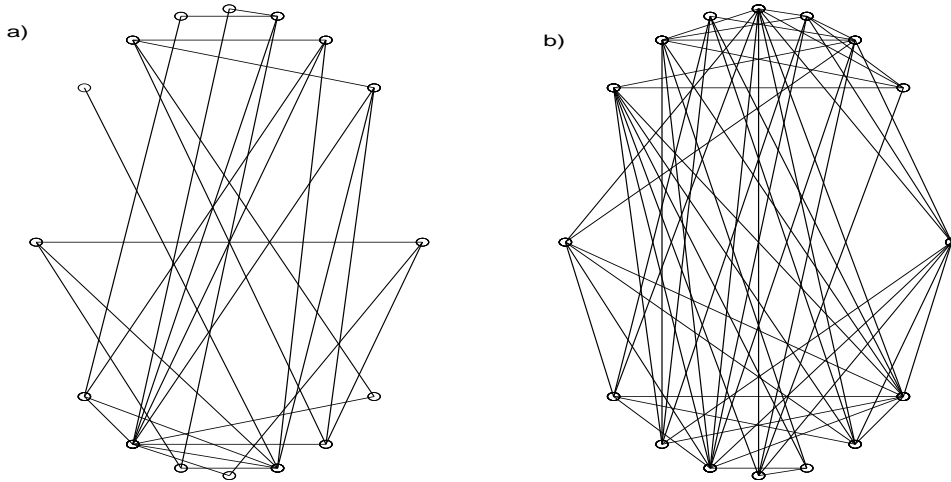


Figure 3: The Erdős and Rényi random graph with $N = 16$. a) $p_{ER} = 0.25$ b) $p_{ER} = 0.5$

Watts and Strogatz (1998) [19] algorithm for the construction of networks is as follows: one-dimensional ring lattice of N nodes connected to its $2K$ nearest neighbors (K is known as the coordination number) and periodic boundary conditions are preselected. The algorithm goes through each of the edges in turn and, independently with probability p_{WS} , “rewires” it to a randomly selected node. That is, the WS algorithm shifts one end of the edge to a new randomly chosen node from the whole lattice (except that no two nodes can have more than

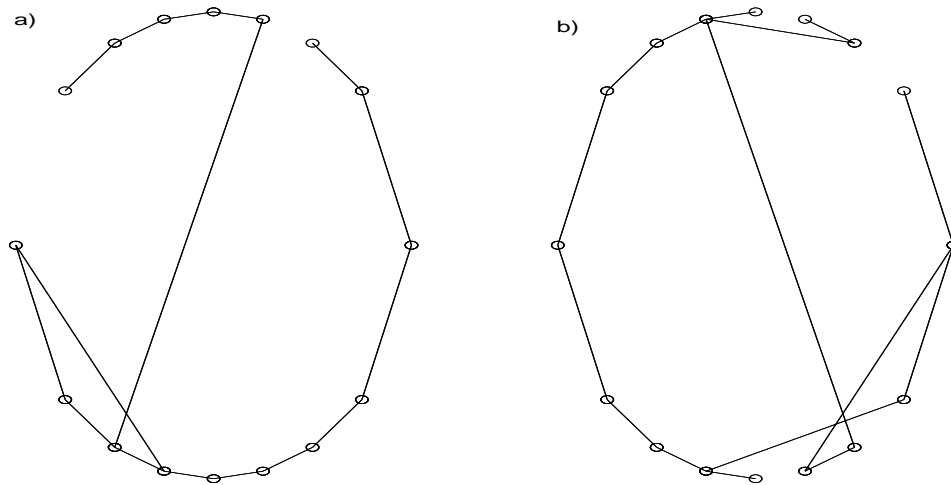


Figure 4: Small-world networks with $N = 16$, $K = 1$, a) $p = 0.1$ b) $p = 0.3$

one edge running between them, and no node can be connected by an edge to itself (see Figure 13). Watts and Strogatz [19] classified networks by their level of randomness, as measured by their own disorder parameter p_{ws} (from “regular” $p_{ws} = 0$ to completely random, $p_{ws} = 1$). Whenever each node in a network is just connected to its nearest two neighbors one on its right and on the other on its left, the network is *regular* [19]. A completely random network has $p_{ws} = 1$, that is, all nodes are randomly connected to each other. Watts and Strogatz showed that the introduction of a small number of random connections ($p \simeq 0.01$) significantly reduces the average distance between any two nodes (characteristic path length), a property that facilitates disease spread. In fact, Watts and Strogatz showed that such average distance grows like $O(\log(N))$ and not as $O(N)$. Networks constructed via the WS algorithm also support high levels of clustering. The small-world effect (short average distance between nodes and high levels of clustering) has been detected in networks that include a network of actors in Hollywood, the power generator network in the western US, and the neural network of *C.elegans* [19]. This

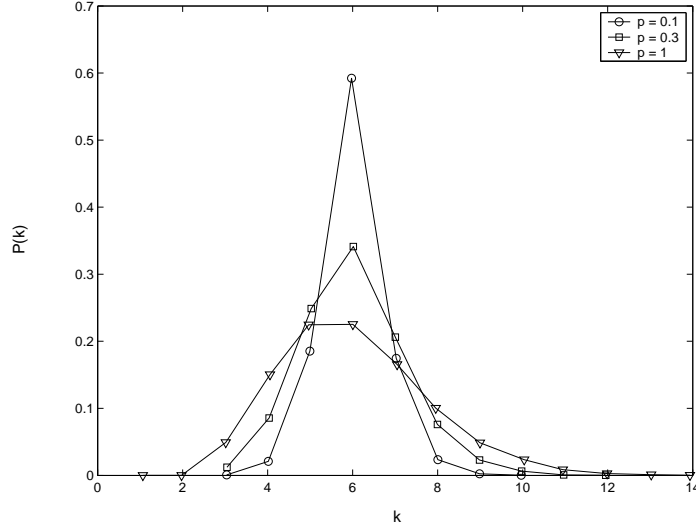


Figure 5: Connectivity distributions $P(k)$ of the small-world network model with three different disorder parameters $p = 0.1$, $p = 0.3$, and $p = 1$ with networks of size 10^4 and $K = 3$.

“small-world effect” had already been documented by the psychologist Stanley Milgram using data from the letter-passing experiments that he conducted in the 1960s [17]. Newman and Watts [31] studied a slight variation of the Watts-Strogatz model. They added shortcut edges with probability ϕ per edge in the underlying ring lattice instead of ‘rewiring’ the existing edges. The Newman and Watts model turned out to be easier to analyze since the network cannot become disconnected after rewiring. Figure 6 shows a small-world network with $N = 16$, $K = 1$ and $\phi = 0.1$. The degree or connectivity distribution of the small-world network model depends on the disorder parameter p . That is, $p = 0$, implies that the connectivity distribution is given by the delta function $\delta(k - 2K)$ where K is the coordination number in the network. As p approaches 1, the connectivity distribution converges to that obtained from the Erdős and Rényi model. Figure 5 shows the degree distribution for a small-world model as a function of

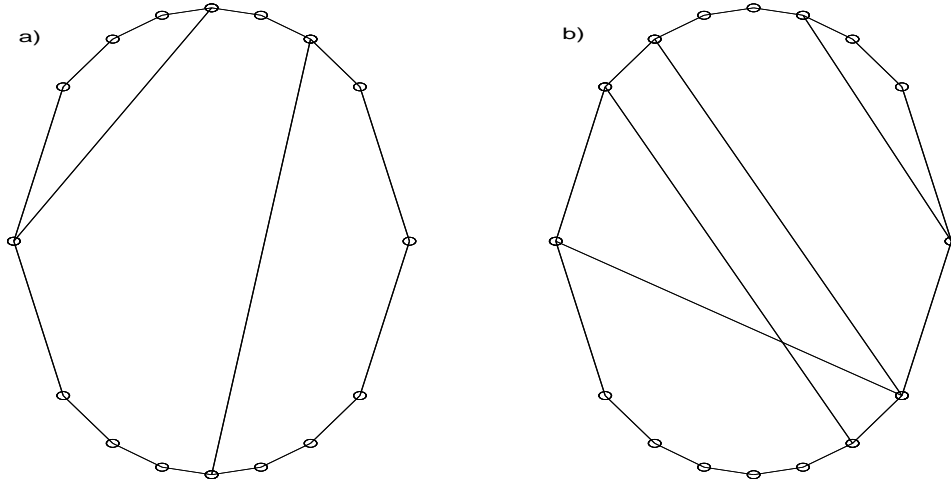


Figure 6: Small-world networks with $N = 16$, $K = 1$, a) $\phi = 0.1$ b) $\phi = 0.3$

the disorder parameter p , when $N = 10^4$ and $K = 3$. “Unfortunately,” small world networks do not exhaust all possibilities. The bell-shaped node degree distributions observed in the Erdős-Rényi, Watts-Strogatz, and Newman-Watts models are in contrast with the power-law degree distributions observed in a number of biological [52], social [20, 21, 24, 32, 33, 47, 51], and technological [20, 21, 53, 55] networks (see Figure 7). [Power-law degree distributions (also known as Pareto distributions) are given by the parametric family:

$$P(k) = Ck^{-\gamma}$$

where γ is typically between 2 and 3 (infinite variance) and C is a normalization constant (makes $P(k)$ a probability density function)]. Networks that fit well power-law degree distributions have a small number of highly connected nodes, that is, most nodes have a small number of connections. Barabási and Albert (1999) dubbed this type of structures *scale-free* networks.

The number of sexual partners in the 1996 Swedish survey of sexual behavior [47] fits a power-

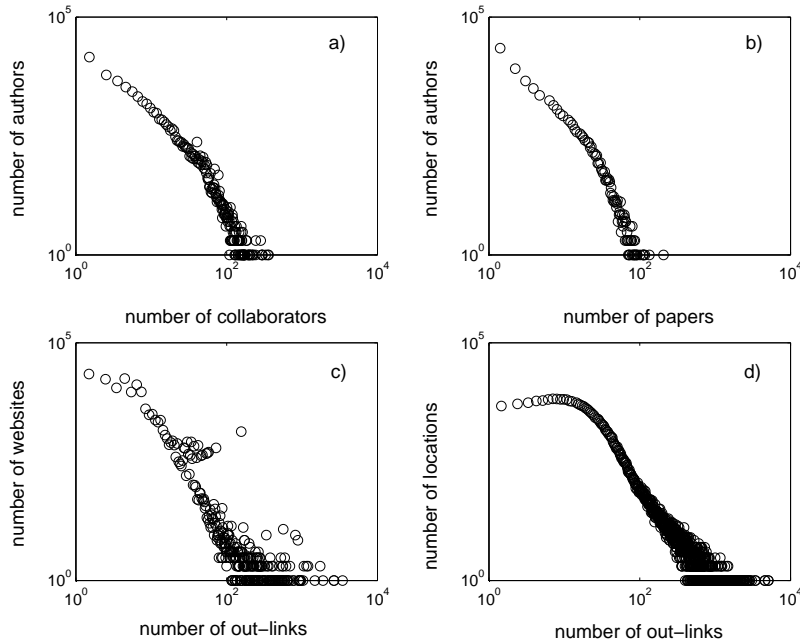


Figure 7: The power-law distributions observed in a,b) Scientific collaboration networks (The Los Alamos e-Print Archive) [56] c) The World-Wide-Web (nd.edu domain) [57] and d) The location-based network of the city of Portland [51].

law distribution and the number of sexual partners of Cornell University undergraduates from the 1990 Cornell Undergraduate Social and Sexual Patterns (CUSSP) survey [50] can also be fitted well by such distribution. These observations, for example, support the view that sex-education campaigns must target individuals with the highest number of partners (core group) [11]. The location-based network of the city of Portland, Oregon also exhibits a scale-free structure (Chowell *et al.* [51]). Here, nodes represent locations while directed connections between locations represent the average movement of individuals in the city. The scale-free (Figure 7(d)) topology implies the existence of a high a number of locations with a low number of

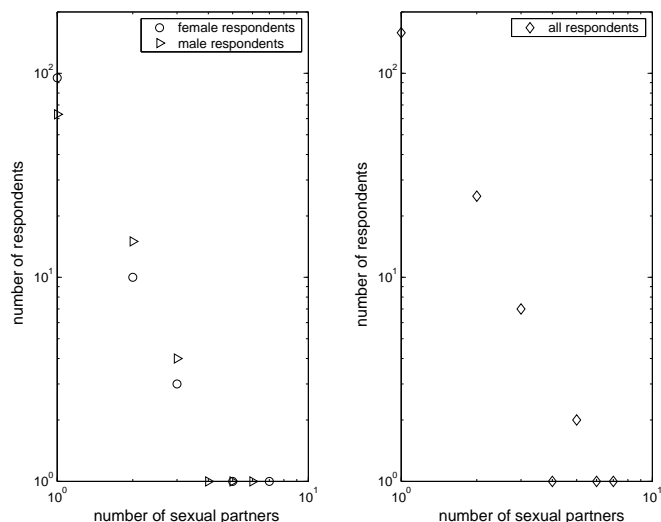


Figure 8: Number of sexual partners of Cornell University undergraduates from the *1990 Cornell Undergraduate Social and Sexual Patterns (CUSSP) survey*[50]. The power-law exponent for females is 2.86, for males is 2.90, and for the overall distribution is 2.78.

connections (i.e households) and a small number of highly connected *hubs* (i.e schools, hospitals, etc.). Barabási and Albert (1999) [20, 21] introduced a simple theoretical model that generates networks with a power-law degree distribution (see Figure 10). The BA algorithm starts with a small number of nodes (m_o) and, at each time step, a new node connects (with m links), with higher probability, to nodes that have already accumulated a higher number of connections. The resulting network has a power-law exponent of 3 and a mean connectivity of $2m$. Thus, the Barabási-Albert (BA) model captures features that seem characteristic of real-world networks, namely, *growth and prefferential attachment*.

Figure 9 shows a network generated using the BA model. Several modifications of the BA model have been studied including edge rewiring [25], edge removal [27], growth constraints

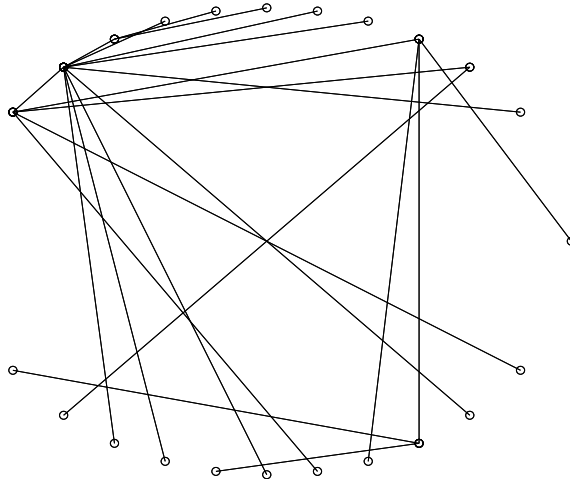


Figure 9: Network of size $N = 23$ generated using the BA model described in the text with $m_o = 2$ and $m = 1$.

[30, 28], and edge competition [29]. Klemrn and Eguíluz (2002) [22] developed an alternative algorithm for the generation of scale-free networks. These researchers incorporated memory as part of a node’s ability to acquire additional links. The Klemrn-Eguíluz model produces scale-free networks with high clustering coefficients, a property not generated by the BA model.

The capacity of networks to maintain essential properties when nodes are removed is a measure of their robustness. In scale-free networks, most of the nodes have low degree, hence their removal “typically” does not impact the connectivity of the remaining vertices. However, the removal of nodes with the highest degree (pressure points) of connectivity can have dramatic consequences (see Figure 11). This effect was first demonstrated independently and numerically by Albert (2000) [26] and Broder (2000) [54] using subsets of data of the World-Wide Web. The practical relevance of network robustness was highlighted by the recent service denial of highly connected web servers including Yahoo, CNN, Amazon, Ebay, Excite and Etrade following a

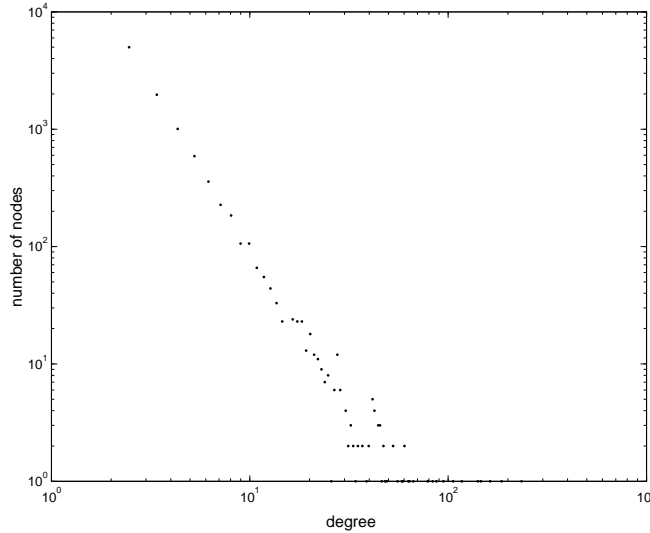


Figure 10: Connectivity distribution of the BA model decays as a power law with $\gamma = 3$. Here, $N = 10000$, $m_o = 3$ and $m = 2$.

network attack.

Important work on the use of worst-case scenarios in the development of response policy has been carried out by Kaplan [12, 13, 14] in the context of HIV and smallpox. However, the nature of his approach does not allow for the incorporation of population structures such as those identified in [20, 21, 24, 32, 33, 51]. The importance and frequency of these networks is the main motivation behind our efforts to look at the rate of growth of epidemic outbreaks on these graphs. The focus of this paper (instigated by Ed Kaplan) is driven by the questions:

** How is the initial rate of epidemic growth affected by a population's structure?*

** What is the role of 'social' topologies and the number of initial infectious sources on the rate*

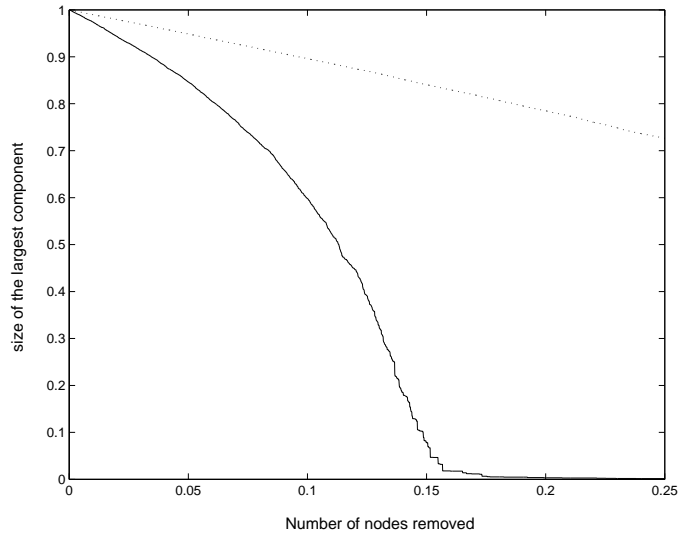


Figure 11: The size of the largest component in a scale-free networks as a function of the number of nodes removed randomly (dashed line) or in decreasing order of degree, that is, hubs are removed first (solid line). The network was constructed using the BA model with $N = 10000$, $m_o = 3$ and $m = 2$.

of growth of an epidemic?

The following sections represent an initial attempt to address these questions in the context of small-world [18, 19] and scale-free networks [20]. The organization of the rest of this paper is as follows: Section II corroborates Kaplan’s view of mixing in worst-case epidemics when the transmission topology is given by small-world networks; Section III focuses on the study of epidemics in scale-free networks where a natural “node” hierarchy often emerges. (This structure, in some sense, “equivalent” to the concept of core group developed by Hethcote and Yorke (1984) [11], seems to provide a fluid landscape for disease spread); Section IV collects

our conclusions, caveats, and views on implications of these results in the study of the impact of deliberate releases of biological agents.

3 Epidemics on small-world networks

Simple epidemic models such as the susceptible-infected-recovered (SIR) model have been studied on small-world networks. Moore and Newman [36] studied SIR epidemics on small world networks via site and bond percolation. In site percolation, nodes (sites) are occupied (by spins) or not and any two spins occupying nearest neighbour sites are connected by an open bond. In bond percolation, the relevant entities are bonds or edges. Bonds are sequentially visited and set open with probability p or closed with probability $1 - p$ (independently). The percolation threshold is the smallest probability p at which an infinite cluster of sites emerges when sites or bonds (depending on the type of percolation) are occupied with that probability. SIR epidemic processes are built on the assumption that nodes are occupied by individuals which can be infected by neighbors connected by edges or bonds (Grassberger [37], 1983). When the total probability of transmission from one individual to another is greater than this threshold, the disease explodes, that is, a “giant” component (whose size is the size of the epidemic) appears [38, 39]. In an epidemic that starts with a single infectious source and spreads as a bond percolation process, the subset of nodes (individuals) that can be reached from the initial infective individuals by traversing only open bonds, is the size of the epidemic outbreak. Newman [35] studied SIR epidemics on a two-dimensional small world network via bond percolation. His results were motivated by the study of disease transmission in plants coming from two sources:

from nearest neighbor (plants) and long-distance contacts (vectors). Epidemics on small-world networks can exhibit phase transition behavior, that is, there is a critical value of the disorder parameter (p_c) such that for values of $p > p_c$ self-sustained oscillations in the number of infected individuals in susceptible-infected-susceptible (SIS) epidemics are possible (Kuperman *et al.* [40]).

In order to study the role of the disorder parameter p (small-world networks) on the initial rate of growth of disease spread, the following algorithm is used to compute its initial (empirical) rate of growth. The number of infected individuals is computed as a function of time $I(t)$ (time is discrete) for a small time range ($t < t_c$). The value of t_c is selected so that $I(t)$ is still in its exponentially growing phase. The algorithm follows three steps:

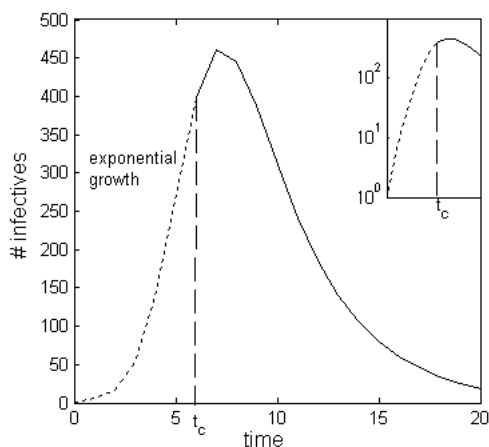


Figure 12: Computation of the empirical rate of growth of epidemics on networks.

1. *Computation of t_c .* The time t_c at which $I(t)$ changes concavity, that is, the value of t at which the second derivative of $I(t)$ changes from positive to negative (see Figure 12).

2. *Rescaling of $I(t)$.* $\hat{I}(t) \equiv \log_e[I(t)]$ for $t < t_c$ where t_c is the value computed in Step 1.

3. *Regression on $\hat{I}(t)$.* Compute the average slope r of the best fitting line to $\hat{I}(t)$. r is the average “r” that results from 50 realizations. The average initial rate of growth r is computed as a function of the disorder parameter (p) of small-world networks ($p \in [0, 1]$ is changed in increments of 0.01).

3.1 Epidemiological model

We consider an stochastic SIR epidemiological model. Hence, individuals can be in one of three epidemiological states: Suceptible (S), infected (I), or recovered (R). A susceptible individual in contact with i infectious individuals may become infected in a short period of time δt with a probability given by $\hat{\beta}i\delta t$ where $\hat{\beta}$ is the constant risk of infection per unit of time and $\delta t = 1$ in this discrete time model. Similarly, infected recover with a probability given by $\hat{\gamma}\delta t$ where $\frac{1}{\hat{\gamma}}$ is the mean period of infectivity. After recovery, individuals get full immunity to the disease.

Epidemics were simulated on small-world networks of size $N = 10^3$ with $K = 2$, $K = 3$, and $K = 5$ (K is the coordination number of small-world networks). Empirical results on the average rate of growth were obtained from the mean of 50 realizations with disease parameters $\hat{\beta} = \frac{4}{7}$ and $\hat{\gamma} = \frac{2}{7}$. Simulations were started by placing randomly a single infectious source. The average rate of growth increases in a nonlinear fashion as the disorder in the network grows.

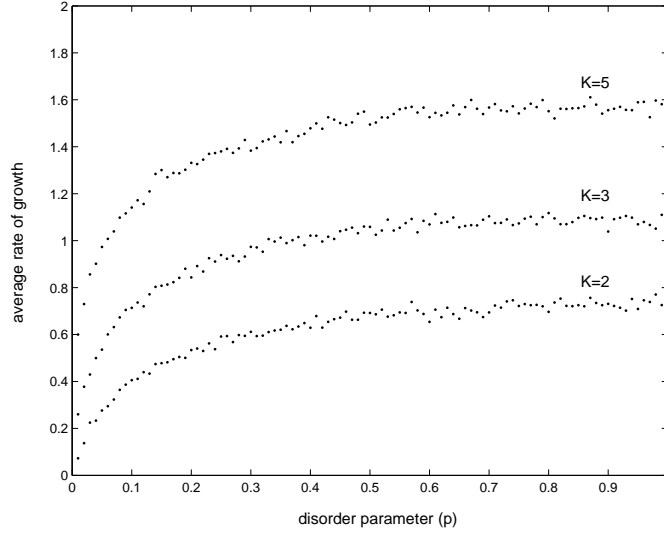


Figure 13: Rate of growth of epidemics in small-world networks of size $N = 10^4$ with $K = 2$, $K = 3$, or $K = 5$, and as a function of the disorder parameter $p \in [0, 1]$. Averages are taken from 50 realizations. p is incremented by 0.01. Disease parameters are: $\hat{\beta} = \frac{4}{7}$, $\gamma = \frac{2}{7}$ and $I(0) = 1$

It saturates when it is close to 1 (totally random networks) with $r_{random} \approx 0.7481$ and $K = 2$. Figure 13 shows the average (from 50 realizations) rate of growth of epidemics in small-world networks of size $N = 10^3$ (with $K = 2$, $K = 3$, and $K = 5$) as a function of the disorder parameter p . The rate of growth in small-world networks also increases as the coordination number (K) increases.

The initial rate of growth of epidemics depends on the network topology. The simulations start with an initial (small) group of infective individuals chosen from those with the highest connectivity. The resulting rate of growth is computed and compared to that resulting from epidemics where the initial infectious sources are chosen (uniformly) at random. Naturally,

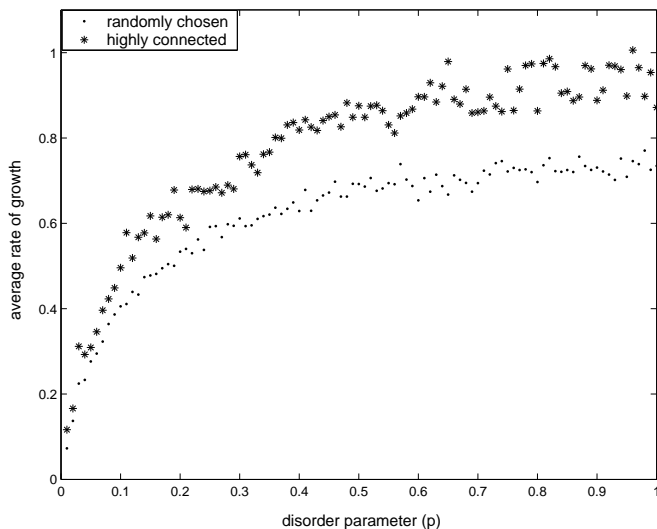


Figure 14: Rate of growth is higher when the epidemics start at the individuals (nodes) with the highest connectivity (*) rather than chosen uniformly at random (.) with $N = 10^4$ and $K = 2$. Averages are taken from 50 realizations. Disease parameters are: $\hat{\beta} = \frac{4}{7}$, $\gamma = \frac{2}{7}$ and $I(0) = 1$.

epidemics that started at the most connected nodes exhibited a higher average rate of growth (see Figure 14). Higher rates of growth are observed as the number of initial infectious sources (always small compared to the size of the network) in the network increases (see Figure 15).

4 Epidemics on scale-free networks

Pastor-Satorras and Vespignani [42] studied a SIS epidemic model on scale-free networks (generated using the BA model) and found that the disease may persist independently of its transmissibility. That is, the *basic reproductive number* R_o , routinely computed in classical mathematical

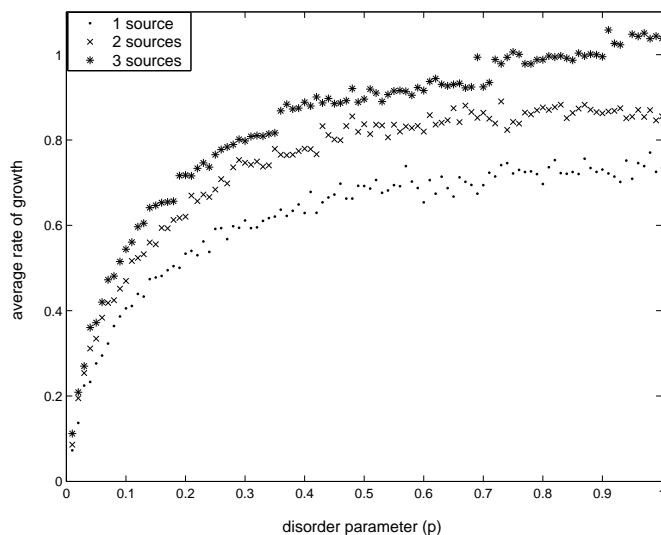


Figure 15: Average rate of growth of multiple source epidemics: one source [$I(0) = 1$] (\cdot), two sources [$I(0) = 2$] (\times) and three sources [$I(0) = 3$] ($*$) with $N = 10^4$ and $K = 2$. Averages are taken from 50 realizations. Disease parameters are: $\hat{\beta} = \frac{4}{7}$, $\gamma = \frac{2}{7}$.

epidemiology, sometimes loses its meaning in their setting. The small number of nodes with a high connectivity (*hubs*) observed in scale-free networks are responsible for “zero” threshold behavior. This observation gives rise to the following question: Can a control strategy be implemented that restores a positive epidemic threshold ?

This question was studied by Pastor-Satorras and Vespignani [43] and independently by Dezsó and Barabási [46]. Both groups concluded that targeted immunization campaigns towards the most connected nodes or hubs increase the probability of recovering finite epidemic threshold behavior. A similar result has been observed on the spread of foot and mouth disease (FMD) in three distinct regions of Uruguay (Rivas *et al.* [44]). A contrasting result has been established on alternative highly clustered scale-free networks [22]. Here, a finite epidemic threshold has

been observed on (SIS) epidemics (Eguíluz and Klemrn [23]).

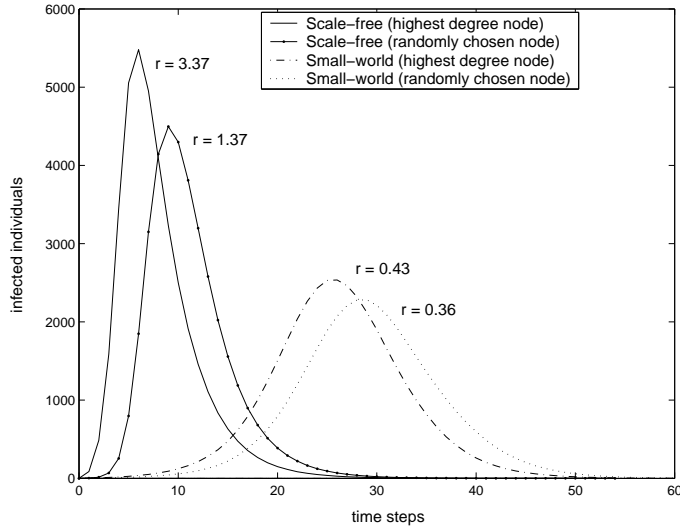


Figure 16: Average number of infected individuals from 50 realizations over time in small-world ($p = 0.1$) and scale-free networks of the same size ($N = 10^4$) and average connectivity ($\bar{k} = 4$). Two different initial conditions are considered: The initial infectious source is placed in a randomly selected or in the most connected node (highest degree). The rates of growth of the epidemics are higher in scale-free networks. Disease parameters are: $\hat{\beta} = \frac{4}{7}$, $\gamma = \frac{2}{7}$ and $I(0) = 1$.

An extensive number of simulations has been carried out of SIR epidemics on scale-free networks. We compute the average rate of growth from the mean of 50 realizations of the epidemic process with two sets of initial conditions: We place the infective source at a randomly selected node or at the most connected node (highest degree). Simulations are carried out on small-world and scale-free networks of the same size ($N = 10^4$) and average connectivity ($\bar{k} = 4$). Significantly higher rates of growth are observed in scale-free networks (see Figure 16). Hence,

scale-free topologies seem to provide ideal scenarios for the study of *worst-case epidemics*. The existence of highly connected nodes or *hubs* in scale-free networks plays a central role on the rate at which viruses (or information) spreads. Or, in other words, the concept of core group [11], is still critical to disease spread on topologically defined networks.

5 Conclusions and caveats

The development and implementation of policies that deal with the deliberate release of biological agents must consider worst possible situations and such scenarios are highly dependent on the network of individual interactions (social topology). Hence, gaining some understanding of the nature of the topological social structures that facilitate disease spread is critical. Kaplan *et al.* [14] assumes that random mixing corresponds to a worst-case scenarios and (using such a set up) concludes, in the case of a smallpox bio-terrorist attack, that mass vaccination, is a better policy than ring vaccination. Halloran *et al.* [15] using a stochastic model with a structured community of 2000 people conclude that targeted vaccination outperforms mass vaccination. The disagreement in results may be directly related to the pre-assumed population structure and mixing topology (network of interactions).

Here, we have tried to identify under what conditions random mixing can be used to model worst-case scenarios. We have found that on small-world networks, random mixing, indeed supports *epidemics* with the highest average rate of growth. However, this is not necessarily the case on scale-free networks. The nature of the mixing between individuals (the connectivity hierarchy in scale-free networks) plays a key role on the initial average rate of growth of an

initial epidemic outbreak. The inherent connectivity hierarchy of scale free networks and the “sensitivity” (lack of robustness) to the removal of key nodes (most connected individuals), in some sense, corresponds to the concept of core group [11]. Highly connected nodes are pressure points in the network and, consequently, their identification and management must be considered in the development and implementation of a logistic plan of response to the threat of a bio-terrorist attack.

The location-based network of the simulated city of Portland possess scale-free nature (Chowell *et al.* [51]). Hence, the initial rate of growth of epidemics in this city can be expected to be (on the average) significantly higher whenever a source is placed at a hub (see Figure 16).

While the use of classical epidemiological approaches has been and will continue to be central in the study of disease spread [1, 2, 3]. It is clear that the study of the potential initial impact of the deliberate release of pathogens on unsuspecting populations must be addressed on various setups. The reasons for such an approach are multiple, the interest is no longer on long-term disease dynamics but on the elaboration of policies that result on timely responses (see Rivas *et al.* [44]). Such a degree of urgency requires the identification of the most sensitive points of release (pressure points) and the use of models that account for multiple releases. The approach used here has its own drawbacks. The most important comes from the fact that temporal dynamics are not explicitly considered. The incorporation of temporal dynamics on networks poses challenges and opportunities for serious theoretical work. Although, we have fell short in addressing the challenge posed by Ed Kaplan, we hope that our results have at

least helped clarify it because the development of contingency plans in worst-case scenarios is fundamental.

References

- [1] R. M. Anderson and R. M. May, *Infectious Diseases of Humans*, Oxford University Press (1991).
- [2] F. Brauer, C. Castillo-Chavez, *Mathematical Models in Population Biology and Epidemiology*, Springer Verlag New York (2000).
- [3] C. Castillo-Chavez with S. Blower, P. van den Driessche, D. Kirschner, and A.-A. Yacubu, *Mathematical Approaches for Emerging and Re-emerging Infectious Diseases Part I: An Introduction to Models, Methods, and Theory; Part II: Models, Methods, and Theory*. Springer (2002).
- [4] O. Diekmann, J. Heesterbeek, *Mathematical Epidemiology of Infectious Diseases: Model Building, Analysis and Interpretation*, John Wiley & Sons (2000).
- [5] Castillo-Chavez C., Z. Feng and W. Huang, *On the computation R_0 and its role on global stability*, *Mathematical Approaches for Emerging and Reemerging Infectious Diseases: An Introduction*, IMA Volume 125, 229-250, Springer-Verlag, Berlin-Heidelberg-New York.
- [6] A. Nold, *Heterogeneity in Disease Transmission*, *Math. Biosci.* 52 227-240 (1980).

- [7] S. Busenberg and C. Castillo-Chavez, *Interaction, Pair Formation and Force of Interaction Terms in Sexually Transmitted Diseases*, Mathematical and Statistical Approaches to AIDS Epidemics (1990).
- [8] C. Castillo-Chavez, J.X. Velasco-Hernandez, and S. Fridman, *Modeling Contact Structures in Biology*, Frontiers of Theoretical Biology, Lecture Notes in Biomathematics, S. A. Levin (ed). 100 454-91 (1994).
- [9] C. Castillo-Chavez and A. Yakubu, *Intra-specific competition, dispersal and disease dynamics in discrete-time patchy environments*, Mathematical Approaches for Emerging and Reemerging Infectious Diseases: An Introduction, IMA Volume 125, 165-181, Springer-Verlag, Berlin-Heidelberg-New York.
- [10] C. Castillo-Chavez, A. Yakubu, H. Thieme, M. Martcheva, *Nonlinear mating models for populations with discrete generations*, Mathematical Approaches for Emerging and Reemerging Infectious Diseases: An Introduction, IMA Volume 125, 165-181, Springer-Verlag, Berlin-Heidelberg-New York.
- [11] H.W. Hethcote and J.A. Yorke, *Gonorrhea Transmission Dynamics and Control*, Lecture Notes in Biomathematics 56, Springer, Berlin, 1984, 105 pages, ISBN 0-387-13870-6.
- [12] E. H. Kaplan, *Asymptotic worst-case mixing in simple demographic models of HIV/AIDS*, Math. Biosci. 108 141-56 (1992).
- [13] E. H. Kaplan, *Mean-max bounds for worst-case endemic mixing models*, Math Biosci. 105 97-109 (1991).

- [14] E. H. Kaplan, D. Craft, and L. Wein, "*Emergency Response to a Smallpox Attack: The Case of Mass Vaccination*", Proceedings of the National Academy of Sciences (2002).
- [15] M. E. Halloran, I. M. Longini, Jr. A. Nizam, and Y. Yang, *Containing Bioterrorist Smallpox*, Science 298: 1428-1432 (2002).
- [16] B. Bollobás, *Random Graphs* (1985) (Academic, London).
- [17] S. Milgram, *The small world problem*, Psychol. Today 2,60-67 (1967).
- [18] S.H. Strogatz, *Exploring Complex Networks*, Nature 410, 268-276 (2001).
- [19] D. J. Watts and S. H. Strogatz, *Collective Dynamics of 'small-world' networks*, Nature 383, 440-442 (1998).
- [20] A.-L. Barabási and R. Albert, *Emergence of Scaling in Random Networks*, Science 286, 509-512 (1999).
- [21] A.-L. Barabási, R. Albert, H. Jeong, *Mean-field theory for scale-free random networks*, PHYSICA A 272 173-87 (1999).
- [22] K. Klemrn and V. M. Eguíluz, *Highly clustered scale-free networks*, Phys. Rev. E 65, 036123 (2002).
- [23] V. M. Eguíluz and K. Klemrn, *Epidemic threshold in structured scale-free networks*, Phys. Rev. Lett. 89, 108701 (2002).
- [24] A.-L. Barabasi, H. Jeong, R. Ravasz, Z. Nda, T. Vicsek, and A. Schubert, *On the topology of the scientific collaboration networks*, Physica A 311, 590-614 (2002).

- [25] Albert R., and A.-L. Barabási, *Topology of evolving networks: Local events and universality*, Physical Review Letters 85, 5234 (2000).
- [26] R. Albert, H. Jeong, and A.-L. Barabási, *Diameter of the World Wide Web*, Nature 401, 130-131 (1999).
- [27] S.N. Dorogovtsev and J.F.F. Mendes, *Language as an evolving Word Web*, Proc. Royal Soc. London B 268, 2603-2606 (2001).
- [28] S.N. Dorogovtsev and J.F.F. Mendes, *Scaling properties of scale-free evolving networks: Continuous approach*, Phys. Rev. E 63, 056125 1-19 (2001).
- [29] G. Bianconi, and A.-L. Barabási, *Competition and multiscaling in evolving networks*, Europhys. Lett. 54 436 (2001).
- [30] Amaral, L. A. N., A. Scala, M. Bartélémy, and H. E. Stanley, *"Classes of Small-World Networks"*, Proc. Natl. Acad. Sci. U.S.A 97, 21 (2000).
- [31] M. E. J. Newman and D. J. Watts, *Renormalization group analysis of the small-world network model*, Phys. Lett. A 263, 341-346 (1999).
- [32] M. E. J. Newman, *The Structure of Scientific Collaboration Networks*, Proc. Natl. Acad. Sci. 98, pp. 404-409 (2001).
- [33] M. E. J. Newman, *Who is the best connected scientist? A study of scientific coauthorship networks*, Phys Rev. E64 (2001) 016131; Phys.Rev. E64 (2001) 016132.

- [34] M. E. J. Newman, *The spread of epidemic disease on networks*, Phys. Rev. E 66, 016128 (2002).
- [35] M. E. J. Newman, *Percolation and epidemics in a two-dimensional small world*, Phys. Rev. Lett. 66, 021904 (2002).
- [36] C. Moore and M. E. J. Newman, *Epidemics and percolation in small-world networks*, Phys. Rev. Lett. 61, 5678-5682 (2000).
- [37] P. Grassberger, *On the critical behavior of the general epidemic process and dynamical percolation*, Math. Biosc. 63, 157-172 (1983).
- [38] D. Stauffer and A. Aharony, *Introduction to Percolation Theory*, Revised 2nd Edition, 2002.
- [39] R. Durrett, *Ten Lectures on Particle systems*, Lecture Notes in Math., 1608, 97-201 (1995).
- [40] M. Kuperman and G. Abramson, *Small-world effect in an Epidemiological model*, Phys. Rev. Lett. 86, 2909-2912 (2001).
- [41] C. P. Warren, L. M. Sander, and I. Sokolov, *Firewalls, disorder, and percolation in epidemics*, cond-mat/0106450.
- [42] R. Pastor-Satorras and A. Vespignani, *Epidemic spreading in scale-free networks*, Phys. Rev. Lett. 86, 3200 (2001).
- [43] R. Pastor-Satorras and A. Vespignani, *Immunization of complex networks*, Phys. Rev. Lett. 65, 036104 (2002).

- [44] A. L. Rivas, S. E. Tennenbaum, J. P. Aparicio, A. L. Hoogesteyn, R. W. Blake, C. Castillo-Chavez, *Critical response time (time available to implement effective measures for epidemic control): Model Building and Evaluation*, to appear in Canadian Journal of Veterinary Research.
- [45] R. M. May and A. L. Lloyd, *Infection dynamics on scale-free networks*, Phys. Rev. Lett. 64, 066112 (2001).
- [46] Z. Dezso and A.-L. Barabási, *Halting viruses in scale-free networks*, Rev. Lett. 65, 055103 (2002).
- [47] F. Liljeros, C.R. Edling, L. A. N. Amaral, H. E. Stanley, and Y. Aberg, *The web of human sexual contacts*, Nature (London) 411, 907 (2001).
- [48] G. Chowell, C. Castillo-Chavez, and S.-F. HSU SCHMITZ, *Power laws in the distribution of the number of sexual partners in the 1990 Cornell Undergraduate Social and Sexual Patterns (CUSPP) survey*, manuscript (2002).
- [49] S. P. Blythe & C. Castillo-Chavez, Nature 344 202 (1990).
- [50] C. M. Crwaford, S. J. Schwager, and C. Castillo-Chavez, *Research design for the Cornell undergraduate social and sexual patterns survey*, Technical report HSS-90-CC1/BU-1083-M, Human Service Studies, Cornell University, Ithaca, New York.

- [51] G. Chowell, J. M. Hyman, S. Eubank, C. Castillo-Chavez, *Analysis of a Real-World Network: The City of Portland*, Los Alamos Unclassified Report LA-UR-02-6658, BSCB department Report BU-1604-M, Cornell University (2002).
- [52] H. Jeong, B. Tombor, R. Albert, Z.N. Oltvai, and A.-L. Barabási, *The large-scale organization of metabolic networks*, Nature 407, 651-654 (2000).
- [53] Ravi Kumar, Prabhakar Raghavan, Sridhar Rajagopalan, D. Sivakumar, Andrew S. Tomkins, Eli UpfalProc (200). 19th ACM SIGACT-SIGMOD-AIGART Symp. Principles of Database Systems, PODS.
- [54] A. Broder, R. Kumar, F. Maghoul, P. Raghavan, S. Rajagopalan, R. Stata, A. Tomkins, J. Wiener, *Graph structure in the web*, 9th International World Wide Web Conference (2000).
- [55] M. Faloutsos, P. Faloutsos, C. Faloutsos, *On Power-Law Relationships of the Internet topology*, SGC0MM (1999).
- [56] <http://www.nd.edu/networks/database/index.html>
- [57] <http://www.santafe.edu/mark/collaboration/>